
Domain Generalization using Causal Matching

Divyat Mahajan
Microsoft Research
Bangalore, India
divyatmahajan@gmail.com

Shruti Tople
Microsoft Research
Cambridge, United Kingdom
shtople@microsoft.com

Amit Sharma
Microsoft Research
Bangalore, India
amshar@microsoft.com

Abstract

Learning invariant representations has been proposed as a key technique for addressing the domain generalization problem. However, the question of identifying the right conditions for invariance remains unanswered. In this work, we propose a causal interpretation of domain generalization that defines domains as interventions under a data-generating process. Based on a general causal model for data from multiple domains, we show that prior methods for learning an invariant representation optimize for an incorrect objective. We highlight an alternative condition: inputs across domains should have the same representation if they are derived from the same base object. In practice, knowledge about generation of data or objects is not available. Hence we propose an iterative algorithm called MatchDG that approximates base object similarity by using a contrastive loss formulation adapted for multiple domains. We then match inputs that are similar under the resultant representation to build an invariant classifier. We evaluate MatchDG on rotated MNIST, Fashion-MNIST, and PACS datasets and find that it outperforms prior work on out-of-domain accuracy and learns matches that have over 25% overlap with ground-truth object matches in MNIST and Fashion-MNIST. Code repository can be accessed here: <https://github.com/microsoft/robustdg>

1 Introduction

Machine learning models are often deployed in applications where the test (inference time) data distributions differ from their training dataset. For example, a model trained on data from one hospital is used for prediction at other hospitals or an image classification model is trained and deployed on pictures with slightly different orientations. These applications require that a model generalizes well to new data distributions in addition to the training distribution, unlike standard machine learning tasks that focus on minimizing same-distribution error. One approach for generalizing to unseen domains is to learn representations that remain invariant across domains, by enforcing that their distributions stay the same across domains, either marginally [1, 2, 3] or conditional on the class label [4, 5, 6]. Other methods frame invariance in terms of accuracy of the classifier on different domains [7, 8]. However, it is unclear how to evaluate these different invariance conditions for their applicability, e.g., under class imbalance or other differences between domains.

To this end, we introduce a formal causal framework for the domain generalization task that allows an easy and coherent characterization of the invariance conditions. Specifically, we construct a model for the data generation process that assumes each input is constructed from a mix of inherent (*causal*) and domain-dependent (*non-causal*) features. Building on prior work [9, 10], we consider domain as a special intervention that changes the non-causal features of an input, and posit that an ideal classifier should be based only on the causal features. Using this model, we show that methods based on enforcing same distribution of representations across domains are inconsistent, confirming claims from past work [7, 11, 12]. Furthermore, we show that methods that enforce the same distribution conditional on class label are also insufficient, unless additional assumptions are made.

The same causal model also provides us with the right condition that an invariant representation should satisfy. Our invariance condition depends on a special *object* variable that defines a collection of inputs that share the same causal features. For example, images of the same person from different viewpoints correspond to a single object, and so do images of the same thing in different rotations, color or background. We show that the correct invariance condition is that the learnt representation be the same for each object across domains. When the object variable is available (e.g., in self-collected data or by using dataset augmentation), we propose a matching regularizer for domain generalization that minimizes the distance between representations of the same object across domains.

In practice, however, the underlying objects are not always known or replicated across domains. We therefore propose an approximation of the above invariant condition that uses class as a proxy, under the assumption that inputs from the same class have more similar causal features than those from different classes. Our algorithm, MatchDG has two phases. First, it constructs a representation such that inputs sharing the same causal features are closer to one another, and matches pairs of inputs that are most similar. Second, it uses these learnt matches as a regularizer when building the classifier.

We find that MatchDG outperforms state-of-the-art methods for out-of-domain accuracy on rotated MNIST and Fashion-MNIST, and the PACS datasets. In addition, for the rotated MNIST and Fashion-MNIST where the ground-truth objects are known, MatchDG learns to makes the representation more similar to their ground-truth matches (more than 50% overlap for top-10 matches), even though the method does not have access to them. Our simple class-based approximation of the invariance condition also beats baselines, indicating the importance of enforcing the correct invariance condition.

Contributions. To summarize, our contributions include:

- **Invariance Condition.** We propose an object-invariant condition for learning a common representation for domain generalization and justify its correctness in contrast to previous approaches.
- **Class-conditional approximation.** When object information is not available, we provide an approximation that leads to a simple algorithm using contrastive loss formulation.
- **MatchDG Algorithm.** We provide a novel two-phase learning algorithm that provides state-of-the-art results on domain generalization datasets like PACS and rotated MNIST and Fashion-MNIST.

2 A causal view of the domain generalization problem

We consider a classification task where the learning algorithm has access to i.i.d. data from m domains, $\{(d_i, \mathbf{x}_i, y_i)\}_{i=1}^n \sim (D_m, \mathcal{X}, \mathcal{Y})^n$ where $d_i \in D_m$ and $D_m \subset \mathcal{D}$ is a set of m domains. Each training input (d, \mathbf{x}, y) is sampled from an unknown probability distribution $\mathcal{P}_m(D, X, Y)$. The task of domain generalization is to learn a single classifier that generalizes well to data from unseen domains $d' \notin D_m$ and to new data from the same domains [13]. Thus, the optimum classifier can be written as: $f^* = \arg \min_{f \in \mathcal{F}} \mathbb{E}_{(d, \mathbf{x}, y) \sim \mathcal{P}} [l(y^{(d)}, f(\mathbf{x}^{(d)}))]$, where $(d, \mathbf{x}, y) \sim \mathcal{P}$ over $(\mathcal{D}, \mathcal{X}, \mathcal{Y})$.

However, we only have access to D_m domains during training. The plug-in estimator replaces \mathcal{P} by \mathcal{P}_m following the Empirical Risk Minimization (ERM) principle.

$$f_{ERM} = \arg \min_{f \in \mathcal{F}} \hat{\mathbb{E}}_{S \sim \mathcal{P}_m} [l(y^{(d)}, f(\mathbf{x}^{(d)}))] \quad (1)$$

where $S = (d, \mathbf{x}, y)^n$ is a training data of size $n = \sum_{d \in D_m} n_d$.

Proposition 1. *The ERM estimator from (1) learns the true f^* , as the set of training domains $D_m = \mathcal{D}$ and number of data samples $n \rightarrow \infty$.*

However, when $D_m \subset \mathcal{D}$, ERM can overfit to the training domains. To avoid overfitting, a popular technique is to learn a common feature representation across all training domains that can be subsequently used to train a classifier [1, 2, 3, 4, 5, 6, 14, 15, 16, 17]. Due to a lack of formal definition of the problem, different learning objectives have been proposed, such as minimizing the distributional distance between learnt feature representations from different domains [1, 2, 3] or minimizing the distance between class-conditional feature representations [4, 5, 6]. We provide a causal framework that provides a correct invariant condition needed for domain generalization.

2.1 Data-generating process

Consider a classification task of detecting the type of item or screening an image for a medical condition. To build a classifier, a train set is generated by taking photos. Due to human variability or by design (to take advantage of data augmentation), a photo may be taken at different angles and sometimes the same object may have multiple photos taken. Thus, the process yields different number of images for each class, sometimes with multiple images for the *same object*. In this example, the domain generalization task is to build a classifier that is robust to different views of any new object.

Figure 1a shows a structural causal model (SCM) that describes the data-generating process. Here each view can be considered as a different *domain* D , the label for item type or medical condition as the class Y , and the image pixels as the features X . Photos of the same item or the same person correspond to a common *object* variable [10], denoted by O . To create an image, the data-generating process first samples an object and view (domain) that may be correlated to each other, (shown with dashed arrows). The pixels in the photo are caused by both the object and the view, as shown by the two incoming arrows to X . Separately, the object corresponds to high-level causal features X_C that are common to any image of the same object, which in turn are used by humans to label the class Y .

The above example is typical of a domain generalization problem; a general SCM is shown in Figure 1b. In general, the underlying *object* for each input $\mathbf{x}_i^{(d)}$ may not be observed. Changing the domain can be seen as an intervention: for each observed $\mathbf{x}_i^{(d)}$, there are a set of (possibly unobserved) counterfactual inputs $\mathbf{x}_j^{(d')}$ where $d \neq d'$, such that all correspond to the same object. Analogous to the causal features X_C , we introduce a node for domain-dependent high-level features of the object X_A . For completeness, we also show the true unobserved label of the object which led to its generation as Y_{true} . Like the object O , Y may be correlated with the domain D . Extending the model in [10], we allow that objects can be correlated with the domain conditioned on Y_{true} . As we shall see, considering the relationship of the *Object* node becomes the key piece for developing the invariant condition. We can write the following non-parametric equations corresponding to the SCM.

$$o := g_o(y_{true}, \epsilon_o) \quad \mathbf{x}_c := g_{xc}(o) \quad \mathbf{x}_a := g_{xa}(d, o, \epsilon_{xa}) \quad \mathbf{x} := g_x(\mathbf{x}_c, \mathbf{x}_a, \epsilon_x) \quad y := h(\mathbf{x}_c, \epsilon_y)$$

where g_o, g_{xc}, g_{xa}, g_x and h are general non-parametric functions. The error ϵ_o is correlated with domain d whereas $\epsilon_{xa}, \epsilon_x$ and ϵ_y are mutually independent error terms that are independent of all other variables. Thus, noise in the class label is independent of domain. Since x_c is common to all inputs of the same object, g_{xc} is a deterministic function of o . In addition to these equations, the SCM provides conditional-independence conditions that all data distributions \mathcal{P} must satisfy, through the concept of d-separation and the perfect map assumption [18].

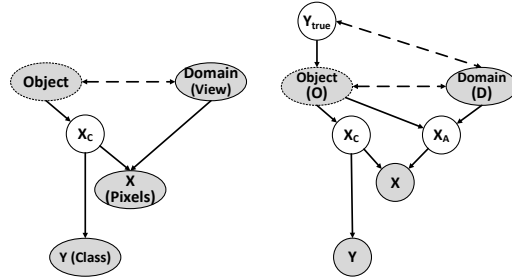
Definition 1. d-separation ([18]): Let A, B, C be the three non-intersecting subsets of nodes in a causal graph \mathcal{G} . For any path between two nodes, a collider is a node where arrows of the path meet head-to-head. A path from A to B is said to be blocked by C if either a non-collider on the path is in C , or there is a collider on the path and neither the collider nor its descendants are in C .

If all paths from A to B are blocked, then A is d-separated from B by C : $dsep(A, B, C) \Rightarrow A \perp\!\!\!\perp B | C$.

2.2 Identifying the invariance condition

From Figure 1b, X_C is the node that causes Y . Further, by d-separation, if we condition on X_C , then the class label is independent of domain, $Y \perp\!\!\!\perp D | X_C$. Thus our goal is to learn y as $h(\mathbf{x}_c)$ where $h: \mathcal{C} \rightarrow \mathcal{Y}$. The ideal loss-minimizing function f^* can be rewritten as (assuming \mathbf{x}_c is known):

$$f^* = \arg \min_f \mathbb{E}_{(d, \mathbf{x}, y)} [l(y, f(\mathbf{x}))] = \arg \min_h \mathbb{E}_{(d, \mathbf{x}, y)} [l(y, h(\mathbf{x}_c))] \quad (2)$$



(a) SCM for image classification example.

(b) General SCM for domain generalization task.

Figure 1: Structural causal models for the data-generating process. Observed variables are shaded; dashed arrows denote correlated nodes. *Object* has a dotted outline since it may not be observed.

Since X_C is unobserved, this implies that we need to learn it too through a representation function $\Phi : \mathcal{X} \rightarrow \mathcal{C}$. Together, $h(\Phi(x))$ leads to the desired classifier $f : \mathcal{X} \rightarrow \mathcal{Y}$.

Conditional independencies from the SCM identify the correct learning goal for learning X_C . By the d-separation criterion, we see that X_C satisfies two conditions: **1)** $X_C \perp\!\!\!\perp D|O$, **2)** $X_C \not\perp\!\!\!\perp O$; where O refers to the object variable and D refers to a domain. The first is an invariance condition: X_C does not change with different domains for the same object. To enforce this, we stipulate that the average pairwise distance between $\Phi(x)$ for inputs across different domains for the same object should be zero, $\sum_{\Omega(j,k)=1; d \neq d'} \text{dist}(\Phi(\mathbf{x}_j^{(d)}), \Phi(\mathbf{x}_k^{(d')})) = 0$. Here $\Omega : \mathcal{X} \times \mathcal{X} \rightarrow \{0, 1\}$ is a *matching* function that is 1 for pairs of inputs across domains corresponding to the same object, and 0 otherwise.

However, just the above invariance will not work: we need the representation to be informative of the object O too (otherwise even a constant Φ minimizes the above loss). Therefore, the second condition stipulates that X_C should be informative of the object, and hence about Y . To ensure informativeness, we can add the standard classification loss, leading to the constrained optimization,

$$f_{\text{perfectmatch}} = \arg \min_{h, \Phi} \sum_{d=1}^m L_d(h(\Phi(X)), Y) \quad \text{s. t.} \quad \sum_{\Omega(j,k)=1; d \neq d'} \text{dist}(\Phi(\mathbf{x}_j^{(d)}), \Phi(\mathbf{x}_k^{(d')})) = 0 \quad (3)$$

where $L_d(h(\Phi(X)), Y) = \sum_{i=1}^{n_d} l(h(\Phi(\mathbf{x}_i^{(d)}), y_i^{(d)}))$. Here f represents the composition $h \circ \Phi$. For example, a neural network with $\Phi(x)$ as its r th layer, and h being the rest of the layers. The proof for the following theorem is in Suppl. A.3.

Theorem 1. For a finite number of domains m , as the number of examples in each domain $n_d \rightarrow \infty$,

1. The set of representations that satisfy the condition $\sum_{\Omega(j,k)=1; d \neq d'} \text{dist}(\Phi(\mathbf{x}_j^{(d)}), \Phi(\mathbf{x}_k^{(d')})) = 0$ contains the optimal $\Phi(\mathbf{x}) = X_C$ that minimizes the domain generalization loss in (2).

2. Further, assuming that $P(X_a|O, D) < \tau < 1$ for every high-level feature X_a that is directly caused by domain, and for P -admissible loss functions [19] whose minimization is the conditional expectation (e.g., ℓ_2 loss or cross-entropy), a loss-minimizing classifier for the following loss is the true function f^* , for some value of λ .

$$f_{\text{perfectmatch}} = \arg \min_{h, \Phi} \sum_{d=1}^m L_d(h(\Phi(X)), Y) + \lambda \sum_{\Omega(j,k)=1; d \neq d'} \text{dist}(\Phi(\mathbf{x}_j^{(d)}), \Phi(\mathbf{x}_k^{(d')})) \quad (4)$$

2.3 Comparison to prior work on learning common representations

Using our model, we now discuss three main representation learning objectives from past work: domain-invariant, class-conditional domain-invariant, and invariant-optimal-classifier representations.

Domain-invariant representations. The goal is to learn a representation Φ such that its distribution $P(\Phi(\mathbf{x}^{(d)}))$ is the same across domains [1, 2, 3], assuming that the ideal representation is independent of domain, $X_C \perp\!\!\!\perp D$. Recent work [7, 11, 12] has argued that this condition fails when Y is correlated with D . However, using d-separation on the SCM from Figure 1b, we find that $Y \perp\!\!\!\perp D$ is not sufficient since O blocks the path between X_C and D . Hence, domain-invariant methods require a stronger condition that both class label and actual objects sampled be independent of domain.

Class-conditional domain-invariant Φ . As a better objective, class-conditional methods [4, 5, 6, 9] aim to obtain representations such that $P(\Phi(\mathbf{x}^{(d)})|Y)$ is the same across domains, through minimizing distribution divergence measures such as the maximum mean discrepancy [4]. However, even in the ideal case where we observe Y_{true} , d-separation on the SCM reveals that $X_C \not\perp\!\!\!\perp D|Y_{\text{true}}$ due to a path through O . Thus, having the same distribution per class is not consistent with properties of X_C .

The above discussion indicates that previous representation learning methods optimize an incorrect objective: even with infinite data across domains, they will not learn the true X_C .

Corollary 1. The conditions enforced by domain-invariant ($\Phi(x) \perp\!\!\!\perp D$) or class-conditional domain-invariant ($\Phi(x) \perp\!\!\!\perp D|Y$) methods are not satisfied by the causal representation X_C . Thus, without additional assumptions, the set of representations that satisfy any of these conditions does not contain X_C , even as $n \rightarrow \infty$.

Invariant-optimal-classifier Φ . Recent work [7, 20] assumes that $P(Y|X_C)$ remains the same across domains and thus a single classifier over the optimal $\Phi(\mathbf{x})$ should be optimal for all domains.

That is, $Y \perp\!\!\!\perp D | \Phi(\mathbf{x})$ which is also satisfied by X_C in the SCM. However, enforcing this condition is difficult in practice and thus the resultant method is restricted to a linear classifier over Φ . In the next section, we propose an alternative condition that supports any architecture, is simple to implement and is also consistent with the SCM.

3 MatchDG: Proposed algorithm

When object information is available, such as in self-collected datasets or when using dataset augmentations, Eq. (4) provided a loss objective to build a classifier based on causal features. In general, however object information is not available. Further, in many datasets there may not be a perfect ‘‘counterfactual’’ match based on same object for an input \mathbf{x} in other domains. Therefore, we now propose a method that aims to learn X_C when no object information is available. We first provide an invariance condition based on observed data that is consistent with the conditional independencies of X_C . We then provide a two-phase contrastive learning method to learn such an X_C .

3.1 An invariant loss consistent with properties of X_C

The object-invariant condition from Section 2.2 can be interpreted as matching pairs of inputs from different domains that share the same X_C . Thus, to approximate it, our goal is to learn a matching $\Omega : \mathcal{X} \times \mathcal{X} \rightarrow \{0, 1\}$ such that pairs having $\Omega(\mathbf{x}, \mathbf{x}') = 1$ have low difference in \mathbf{x}_c and \mathbf{x}'_c . One simple way is to use the class label and match every input to a random input from the same class. This leads to the following *random match* regularizer for learning a classifier:

$$f_{\text{randommatch}} = \arg \min_{h, \Phi} \sum_{d=1}^m L_d(h(\Phi(X)), Y) + \lambda \sum_{\Omega_Y(j,k)=1; d \neq d'} \text{dist}(\Phi(\mathbf{x}_j^{(d)}), \Phi(\mathbf{x}_k^{(d')})) \quad (5)$$

where Ω_Y randomly matches pairs from the same class. Assuming X_C of inputs from the same class is bounded by δ , we show that this simple matching strategy does include X_C as a possible solution.

Theorem 2. *Assume that training domains are diverse such that for any two same-class inputs $\mathbf{x}_j^{(d)}$ and $\mathbf{x}_k^{(d')}$ from domains d and d' , $\text{dist}(x_{a,j}^{(d)}, x_{a,k}^{(d')}) \geq \delta_a$ where x_a is any high-level feature that is caused directly by domain. Further, assume that the distance over X_C between same-class inputs from different domains is bounded: $\text{dist}(x_{c,j}^{(d)}, x_{c,k}^{(d')}) \leq \delta_c$ and $\delta_c < \delta_a$. Then for some λ , a loss-minimizing classifier for the loss from (5) is the true function f^* , given a P -admissible loss function and a finite number of domains m with $n_d \rightarrow \infty$ in each domain.*

The proof substitutes X_C in the match condition and uses Lagrange multipliers, detailed in Suppl. A.5 Compared to class-conditional domain-invariant condition, a key distinction is that we are enforcing the difference in *individual* representations for inputs from the same class to be low, not just that they have the same distribution. That is, we are also minimizing the variance of the class-conditional distribution. A variation of this loss is used as a contrastive regularizer in [21, 22]. However, Theorem 2 cannot provide any guarantee that X_C will be returned by the optimization. The key parameter is δ_c . If a dataset has low δ_c (as compared to distance between inputs of different classes), then there is a high chance of learning a good representation that is close to X_C (if $\delta_c = 0$, we obtain perfect match). But as δ_c increases, the matching condition loses any discriminative power. Therefore we need to learn a matching Ω such that δ_c is minimized.

3.2 MatchDG: Two-phase algorithm with learnt matches

To learn such a Ω , we utilize recent work from unsupervised contrastive learning [23, 24] and adapt it for domain generalization. Our method works on the assumption that two inputs from the same class have more similar causal features than inputs from a different classes. Thus, if we can build a representation where inputs from the same class are comparatively closer, then a matching built on the closest pairs in this representation are more likely to have lower δ_c than a simple class-based random match. Specifically, we optimize a contrastive representation learning loss that minimizes distance between same-class inputs from different domains in comparison to inputs from different classes across domains. Adapting the contrastive loss for a single domain [23], we consider *positive* matches as two inputs with the same class but different domains, and *negative* matches as pairs with

different classes. For every positive match pair $(\mathbf{x}_j, \mathbf{x}_k)$, we propose the following loss where τ is a hyperparameter and $\text{sim}(\mathbf{u}, \mathbf{v}) = \mathbf{u}^T \mathbf{v} / \|\mathbf{u}\| \|\mathbf{v}\|$ is the cosine similarity.

$$l(\mathbf{x}_j, \mathbf{x}_k) = -\log \frac{\exp(\text{sim}(\Phi(\mathbf{x}_j), \Phi(\mathbf{x}_k))/\tau)}{\exp(\text{sim}(\Phi(\mathbf{x}_j), \Phi(\mathbf{x}_k))/\tau) + \sum_{i=0, y_i \neq y_j}^b \exp(\text{sim}(\Phi(\mathbf{x}_j), \Phi(\mathbf{x}_i))/\tau)} \quad (6)$$

Our key insight is that matches can be updated during training. Rather than the standard contrastive loss where matches are pre-decided, we can start training with a random match based on class and then after every t epochs, update the matches based on nearest same-class pairs in representation space, and iterate until convergence. Under assumption that inputs of same class are closer in causal features, optimizing for the initial random matches should lead to a representation wherein similarity correlates more to similarity in causal features. This completes Phase I of the algorithm. In Phase 2, we utilize the final representation to compute a new match function based on closest same-class pairs and then apply (5) to obtain a classifier regularized on those matches. In Suppl. C.5, we compare the gains due to the proposed iterative matching versus standard contrastive training.

To implement MatchDG, we build a $n \times m$ data matrix containing $m - 1$ positive matches for each input and then sample mini-batches from this matrix. The last layer of the contrastive loss network is considered as the learnt representation. Algorithm 1 provides an overview; details are in Suppl. B.1. We implement MatchDG as a 2-phase method, unlike previous methods [21, 22] that employed class-based contrastive loss as a regularizer with ERM. This is to avoid the classification loss interfering with the goal of learning an invariant representation across domains (e.g., in datasets where one of the domains has many more samples than others). Therefore, we first learn the match function using only the contrastive loss. Our results in Suppl. C.3 show that the two-phase method provides better overlap with ground-truth perfect matches than optimizing classification and matching simultaneously.

Algorithm 1: MatchDG

Input: Dataset $(d_i, x_i, y_i)_{i=1}^n$ from m domains, τ, t

Output: Function $f : \mathcal{X} \rightarrow \mathcal{Y}$
 Create random match pairs Ω_Y .
 Build a $n * m$ data matrix \mathcal{M} .

Phase I. while notconverged do

for $batch \sim \mathcal{M}$ **do**

 Minimize contrastive loss (6).

if $epoch \% t == 0$ **then**

 Update match pairs using Φ_{epoch} .

Phase 2. Compute matching based on Φ . Minimize the loss (5) to obtain f .

4 Evaluation

We evaluate MatchDG for classification accuracy and the quality of its generated matches. We compare MatchDG to 3 other training methods: 1) ERM: Standard empirical risk minimization, 2) ERM-RandMatch that implements the loss from Eq. (5), 3) ERM-PerfMatch that has access to object information and uses the loss from Eq. (4) (not for PACS). We use the cross-entropy loss for L_d and ℓ_2 distance for dist in Eq.(4), (5). Details of implementation are in Suppl. B.1. We also evaluate against state-of-the-art methods such as MASF [22], CSD [25] and JiGen [26]. All the numbers are averaged over 3 runs with standard deviation in brackets. We use three domain generalization datasets from prior work: Rotated MNIST [25] and Fashion-MNIST [25], and PACS [27].

Rotated MNIST & Fashion-MNIST. The datasets contain rotations of grayscale MNIST handwritten digits and fashion article images from 0° to 90° with an interval of 15° [16], where each rotation angle represents a domain. Since different domains’ images are generated from the same base image (object), there exist perfect matches across domains. The task is to predict the correct class label out of 10 classes on a new rotation domain. Following past work [25], we report accuracy on 0° and 90° together as the test domain and the rest as the train domains; since these test domains are the hardest to generalize to (being extreme angles not covered in the span of train domains). We use 2000 and 10,000 samples [25] from each domain for rotated MNIST and Fashion-MNIST during training, and train models using a 2-layer [21] and Resnet-18 architecture [25].

PACS. This dataset contains total 9991 images from four domains: Photos (P), Art painting (A), Cartoon (C) and Sketch (S). The task is to classify objects over 7 different classes. Following [22, 26], we train 4 models with each of the domain as the target using Resnet-18 and Alexnet.

Table 1: Accuracy for Rotated MNIST & Fashion-MNIST datasets on target domains of 0° and 90° . Accuracy for CSD and MASF are reproduced from their code [25, 22].

Dataset	Source	ERM	MASF	CSD	ERM-RandMatch	MatchDG	ERM-PerfMatch
Rotated MNIST	15, 30, 45, 60, 75	96.5 (0.15)	93 (0.2)	94.7 (0.2)	97.5 (0.17)	97.5 (0.36)	98.5 (0.08)
	30, 45, 60	80.6 (2.9)	69.4 (1.32)	89.1 (0.004)	82.8 (2.3)	88.9 (2.01)	93.6 (0.53)
	30, 45	64.0 (2.28)	60.8 (1.53)	77.2 (0.04)	69.7 (2.93)	79.3 (4.2)	84.2 (2.33)
Rotated Fashion MNIST	15, 30, 45, 60, 75	78.5 (1.15)	72.4 (2.9)	78.9 (0.7)	80.5 (0.97)	83.5 (1.16)	85.1 (0.97)
	30, 45, 60	33.9 (1.04)	25.7 (1.73)	27.8 (0.01)	35.5 (1.07)	51.7 (2.08)	61.04 (1.33)
	30, 45	21.85 (0.93)	20.8 (1.26)	20.2 (0.01)	23.9 (0.93)	36.6 (2.17)	42.0 (2.42)

Table 2: Overlap with perfect matches. top-10 overlap and the mean rank for perfect matches for MatchDG and ERM over all training domains. Lower is better for mean rank.

Dataset	Method	Overlap (%)	Top 10 Overlap (%)	Mean Rank
MNIST	ERM	16.4 (1.15)	47.3 (1.17)	28.3 (1.25)
	MatchDG (Default)	26.8 (2.49)	58.9 (3.31)	21.4 (2.37)
	MatchDG (PerfMatch)	37.5 (0.23)	70.6 (4.99)	12.8 (2.23)
Fashion MNIST	ERM	2.8 (0.23)	13.5 (0.49)	197.2 (5.89)
	MatchDG (Default)	24.9 (3.43)	51.9 (5.63)	76.1 (14.3)
	MatchDG (PerfMatch)	58.3 (3.71)	85.3 (3.78)	10.5 (2.81)

4.1 Results: Rotated MNIST (rotMNIST) and Fashion MNIST (rotFashionMNIST)

Under different training domains, Table 1 shows classification accuracy on rotMNIST and rotFashionMNIST for test domains 0° and 90° using Resnet-18 architecture. On both datasets, MatchDG *outperforms* all baselines except ERM-PerfMatch which has oracle access to the perfect matches. MatchDG’s accuracy lies between ERM-RandMatch and ERM-PerfMatch, indicating the benefit of learning a matching function. As the number of training domains decrease, the gap between MatchDG and baselines is highlighted: with 3 source domains for rotFashionMNIST, MatchDG achieves accuracy of 51.7% whereas the next best method ERM-RandMatch achieves 35.5%. Interestingly, ERM-RandMatch also performs better than prior work (MASF and CSD) on rotFashionMNIST dataset, suggesting the power of the simple matching condition proposed in this paper. Note that our baseline ERM provides better accuracy than MASF and CSD on rotMNIST dataset for training with 5 domains but not when they are reduced.

We also evaluate on a simpler 2-layer network to compare MatchDG to other prior works [3, 13, 16, 21, 28], and on a more difficult setting when the test domain data is sampled from different base objects than the training domain. Results are in Suppl. C.1, C.2.

Why MatchDG works? We compare the matches returned by MatchDG Phase I (on Resnet-18 network) to the ground-truth perfect matches and find that it has significantly higher overlap than matching based on ERM loss (Table 2). We report three metrics on the representation learnt at the end of Phase I: percentage of MatchDG matches that are perfect matches,

Table 3: Accuracy results using a fraction of perfect matches during training

	MNIST	Fashion-MNIST
Random Match	97.5 (0.17)	80.5 (0.97)
Approx 25%	97.7 (0.33)	82.5 (1.14)
Approx 50%	97.7 (0.29)	83.1 (1.19)
Approx 75%	98.2 (0.16)	83.9 (0.81)
Perfect Match (100%)	98.5 (0.08)	85.1 (0.97)

Table 4: Accuracy results on the PACS dataset trained with Resnet-18.

Test Domain	ERM	MASF	JiGen	CSD	ERM-RandMatch	MatchDG
Photo	95.37 (0.37)	94.99 (0.09)	96.03	95.45	95.59 (0.07)	95.7 (0.52)
Art Painting	75.79 (1.38)	80.29 (0.18)	79.42	79.79	78.58 (0.56)	77.9 (0.61)
Cartoon	77.82 (0.39)	77.17 (0.08)	75.25	75.04	80.02 (1.01)	78.8 (0.29)
Sketch	69.75 (0.58)	71.69 (0.22)	71.35	72.46	76.03 (1.34)	76.3 (0.92)
Average	79.69	81.04	80.41	80.69	82.56	82.03

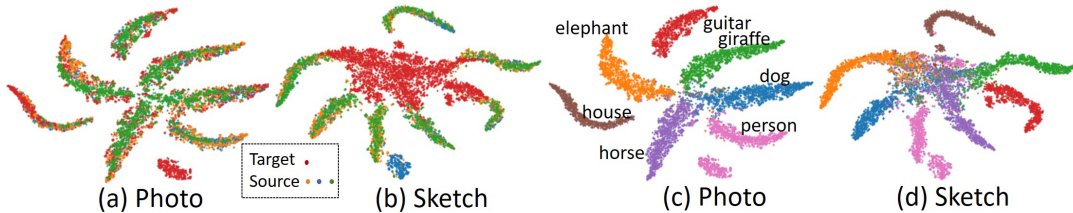


Figure 2: The t-SNE plots for visualizing features learnt in MatchDG Phase 1. (a)-(c) are for Photo as the target domain and (b)-(d) are for Sketch.

percentage of inputs for which the perfect match is within the top-10 ranked MatchDG matches, and mean rank of perfect matches measured by distance over the MatchDG representation.

On all three metrics, MatchDG finds a representation whose matches are more consistent with ground-truth perfect matches. For both rotMNIST and rotFashionMNIST datasets, more than 50% of the inputs have their perfect match within top-10 ranked matches based on the representation learnt by MatchDG Phase I. About 25% of all matches learnt by MatchDG are perfect matches. For comparison, we also show metrics for an (oracle) MatchDG method that is initialized with perfect matches: it achieves even better overall and Top-10 values, indicating the importance of knowing ground-truth matches that can be useful in data augmentation settings. Similar results for MatchDG Phase 2 are in Suppl. C.3. Mean rank for rotFashionMNIST may be higher because of the larger sample size 10, 000 per domain; metrics for training with 2000 samples are in Suppl. C.4.

Finally, to see how the overlap with perfect matches affects classification accuracy, we simulate random matches with 25%, 50% and 75% overlap with perfect matches (Table 3). We find that accuracy increases as the fraction of perfect matches increase. Interestingly, the accuracy for 25% overlap roughly predicts the reported accuracy for MatchDG (which had about 25% overlap). These results confirm that in addition to high accuracy, Phase I of MatchDG allows for learning a representation where inputs with the same causal features are closer.

4.2 PACS dataset: Accuracy and t-SNE plots

On the PACS dataset too, our matching-based methods outperform prior work on classification accuracy averaged over all domains (Table 4). In particular, on the relatively difficult domains of Sketch and Cartoon, MatchDG and ERM-RandMatch achieve the highest accuracies: MatchDG obtains 76.3% on the Sketch domain, an improvement of $\approx 5\%$ from prior state-of-the-art. Results with AlexNet network and comparisons to more prior work [6, 7, 16, 22, 26, 27, 29, 30, 31] are in Suppl. D. Beyond accuracy, we investigate the quality of representations learnt by MatchDG using t-SNE [32] in Figure 2. Comparing the Phase I models for the easiest (Photo) and hardest (Sketch) unseen domains (Figs. 2a,b), we find that MatchDG achieves a higher overlap between train and test domains for Photo than Sketch, highlighting the difficulty of generalizing to the Sketch domain, even as classes are well-separated in the training domains for both models (Figs. 2c,d).

5 Related Work

There are four main approaches for the domain generalization task: learning a common representation, dataset augmentation, meta-learning and sharing common parameters.

Learning common representation. To learn a generalizable classifier, several methods enforce same distribution of $\Phi(\mathbf{x})$ across domains marginally or conditional on class label, using divergence measures such as maximum mean discrepancy [1, 4], adversarial training with a domain discriminator [2, 3, 6], use discriminant analysis [5, 17], and other techniques [16]. In Section 2.3, we identified limitations of the above methods. A more recent line of work [7, 20] enforces domain-invariance of the optimal $P(Y|\Phi(\mathbf{x}))$ that we compare to in the evaluation. There is work on use of causal reasoning for domain adaptation [9, 10, 33, 34] that assumes $Y \rightarrow X$ direction and other work [7, 8] on connecting causality that assumes $X \rightarrow Y$. Our SCM model unites these streams by introducing Y_{true} and labelled Y and develop an invariance condition for domain generalization that is valid under both interpretations. Perhaps the closest to our work is by Heinze-Deml and Meinshausen [10] who use the object concept in generation of input for a single domain but assume that objects are observed. We provide an algorithm that does not depend on observed objects. In doing so, we provide theoretical justification for the past uses of contrastive loss in domain generalization based on the class label [21, 22] or using augmented data [35].

Meta-learning. Meta-learning can be applied to domain generalization, by creating meta-train and meta-test domains within each mini-batch and ensuring that the weight updates perform well on the meta-test domains [22, 29, 30]. While we showed that a contrastive training only can achieve promising results, combining meta-learning with our approach is an interesting future direction.

Dataset augmentation.: The data augmentation methods create more out-of-domain samples, from distributions within a bounded distance [36] or on a continuous space of domain interventions [13].

Parameter Decomposition. Finally there is work that focuses on identifying common model parameters across domains [25, 27, 37], rather than a common input representation. We compared our work against one such recent method based on low-rank decomposition (CSD) [25].

6 Conclusion

We presented a causal interpretation of domain generalization and used it to derive a method that matches representations of input pairs that share causal features. We find that combining ERM with a simple invariance condition performs better on benchmarks than prior work, and hope to investigate matching-based methods with domain-dependent noise on class label and object in future work.

Acknowledgements

We would like to thank Adith Swaminathan, Aditya Nori, Emre Kiciman, Praneeth Netrapalli, Tobias Schnabel, and Vineeth Balasubramanian who provided us valuable feedback on this work. We also thank Vihari Piratla who helped us with reproducing the CSD method and other baselines.

References

- [1] Krikamol Muandet, David Balduzzi, and Bernhard Schölkopf. Domain generalization via invariant feature representation. In *International Conference on Machine Learning*, pages 10–18, 2013.
- [2] Haoliang Li, Sinno Jialin Pan, Shiqi Wang, and Alex C Kot. Domain generalization with adversarial feature learning. In *Proceedings of the IEEE Conference on Computer Vision and Pattern Recognition*, pages 5400–5409, 2018.
- [3] Yaroslav Ganin, Evgeniya Ustinova, Hana Ajakan, Pascal Germain, Hugo Larochelle, François Laviolette, Mario Marchand, and Victor Lempitsky. Domain-adversarial training of neural networks. *The Journal of Machine Learning Research*, 17(1):2096–2030, 2016.
- [4] Ya Li, Mingming Gong, Xinmei Tian, Tongliang Liu, and Dacheng Tao. Domain generalization via conditional invariant representations. In *Thirty-Second AAAI Conference on Artificial Intelligence*, 2018.
- [5] Muhammad Ghifary, David Balduzzi, W Bastiaan Kleijn, and Mengjie Zhang. Scatter component analysis: A unified framework for domain adaptation and domain generalization. *IEEE transactions on pattern analysis and machine intelligence*, 39(7):1414–1430, 2016.

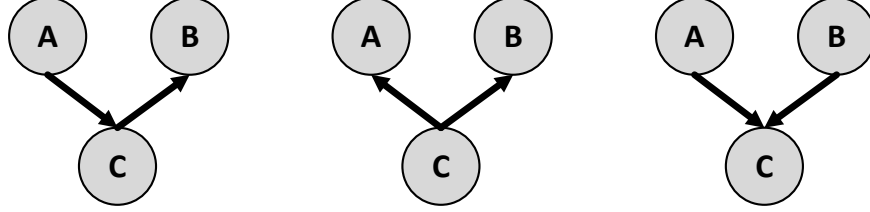
- [6] Ya Li, Xinmei Tian, Mingming Gong, Yajing Liu, Tongliang Liu, Kun Zhang, and Dacheng Tao. Deep domain generalization via conditional invariant adversarial networks. In *Proceedings of the European Conference on Computer Vision (ECCV)*, pages 624–639, 2018.
- [7] Martin Arjovsky, Léon Bottou, Ishaan Gulrajani, and David Lopez-Paz. Invariant risk minimization. *arXiv preprint arXiv:1907.02893*, 2019.
- [8] Jonas Peters, Peter Bühlmann, and Nicolai Meinshausen. Causal inference by using invariant prediction: identification and confidence intervals. *Journal of the Royal Statistical Society: Series B (Statistical Methodology)*, 78(5):947–1012, 2016.
- [9] Mingming Gong, Kun Zhang, Tongliang Liu, Dacheng Tao, Clark Glymour, and Bernhard Schölkopf. Domain adaptation with conditional transferable components. In *International conference on machine learning*, pages 2839–2848, 2016.
- [10] Christina Heinze-Deml and Nicolai Meinshausen. Conditional variance penalties and domain shift robustness. *arXiv preprint arXiv:1710.11469*, 2019.
- [11] Han Zhao, Remi Tachet des Combes, Kun Zhang, and Geoffrey J Gordon. On learning invariant representation for domain adaptation. *arXiv preprint arXiv:1901.09453*, 2019.
- [12] Fredrik D Johansson, David Sontag, and Rajesh Ranganath. Support and invertibility in domain-invariant representations. In *The 22nd International Conference on Artificial Intelligence and Statistics*, pages 527–536, 2019.
- [13] Shiv Shankar, Vihari Piratla, Soumen Chakrabarti, Siddhartha Chaudhuri, Preethi Jyothi, and Sunita Sarawagi. Generalizing across domains via cross-gradient training. In *International Conference on Learning Representations*, 2018.
- [14] Eric Tzeng, Judy Hoffman, Trevor Darrell, and Kate Saenko. Simultaneous deep transfer across domains and tasks. In *Proceedings of the IEEE International Conference on Computer Vision*, pages 4068–4076, 2015.
- [15] Isabela Albuquerque, João Monteiro, Tiago H Falk, and Ioannis Mitliagkas. Adversarial target-invariant representation learning for domain generalization. *arXiv preprint arXiv:1911.00804*, 2019.
- [16] Muhammad Ghifary, W Bastiaan Kleijn, Mengjie Zhang, and David Balduzzi. Domain generalization for object recognition with multi-task autoencoders. In *Proceedings of the IEEE international conference on computer vision*, pages 2551–2559, 2015.
- [17] Shoubo Hu, Kun Zhang, Zhitang Chen, and Laiwan Chan. Domain generalization via multidomain discriminant analysis. In *Uncertainty in artificial intelligence: proceedings of the... conference. Conference on Uncertainty in Artificial Intelligence*, volume 35. NIH Public Access, 2019.
- [18] Judea Pearl. *Causality*. Cambridge university press, 2009.
- [19] John W Miller, Rod Goodman, and Padhraic Smyth. On loss functions which minimize to conditional expected values and posterior probabilities. *IEEE Transactions on Information Theory*, 39(4):1404–1408, 1993.
- [20] Kartik Ahuja, Karthikeyan Shanmugam, Kush Varshney, and Amit Dhurandhar. Invariant risk minimization games. *arXiv preprint arXiv:2002.04692*, 2020.
- [21] Saeid Motiian, Marco Piccirilli, Donald A Adjeroh, and Gianfranco Doretto. Unified deep supervised domain adaptation and generalization. In *Proceedings of the IEEE International Conference on Computer Vision*, pages 5715–5725, 2017.
- [22] Qi Dou, Daniel Coelho de Castro, Konstantinos Kamnitsas, and Ben Glocker. Domain generalization via model-agnostic learning of semantic features. In *Advances in Neural Information Processing Systems*, pages 6447–6458, 2019.
- [23] Ting Chen, Simon Kornblith, Mohammad Norouzi, and Geoffrey Hinton. A simple framework for contrastive learning of visual representations. *arXiv preprint arXiv:2002.05709*, 2020.
- [24] Kaiming He, Haoqi Fan, Yuxin Wu, Saining Xie, and Ross Girshick. Momentum contrast for unsupervised visual representation learning. *arXiv preprint arXiv:1911.05722*, 2019.
- [25] Vihari Piratla, Praneeth Netrapalli, and Sunita Sarawagi. Efficient domain generalization via common-specific low-rank decomposition. *arXiv preprint arXiv:2003.12815*, 2020.
- [26] Fabio M Carlucci, Antonio D’Innocente, Silvia Bucci, Barbara Caputo, and Tatiana Tommasi. Domain generalization by solving jigsaw puzzles. In *Proceedings of the IEEE Conference on Computer Vision and Pattern Recognition*, pages 2229–2238, 2019.
- [27] Da Li, Yongxin Yang, Yi-Zhe Song, and Timothy M Hospedales. Deeper, broader and artier domain generalization. In *Proceedings of the IEEE international conference on computer vision*, pages 5542–5550, 2017.

- [28] Ian J Goodfellow, Jonathon Shlens, and Christian Szegedy. Explaining and harnessing adversarial examples. *arXiv preprint arXiv:1412.6572*, 2014.
- [29] Da Li, Yongxin Yang, Yi-Zhe Song, and Timothy M Hospedales. Learning to generalize: Meta-learning for domain generalization. In *Thirty-Second AAAI Conference on Artificial Intelligence*, 2018.
- [30] Yogesh Balaji, Swami Sankaranarayanan, and Rama Chellappa. Metareg: Towards domain generalization using meta-regularization. In *Advances in Neural Information Processing Systems*, pages 998–1008, 2018.
- [31] Da Li, Jianshu Zhang, Yongxin Yang, Cong Liu, Yi-Zhe Song, and Timothy M Hospedales. Episodic training for domain generalization. In *Proceedings of the IEEE International Conference on Computer Vision*, pages 1446–1455, 2019.
- [32] Laurens van der Maaten and Geoffrey Hinton. Visualizing data using t-sne. *Journal of machine learning research*, 9(Nov):2579–2605, 2008.
- [33] Sara Magliacane, Thijs van Ommen, Tom Claassen, Stephan Bongers, Philip Versteeg, and Joris M Mooij. Domain adaptation by using causal inference to predict invariant conditional distributions. In *Advances in Neural Information Processing Systems*, pages 10846–10856, 2018.
- [34] Mateo Rojas-Carulla, Bernhard Schölkopf, Richard Turner, and Jonas Peters. Invariant models for causal transfer learning. *The Journal of Machine Learning Research*, 19(1):1309–1342, 2018.
- [35] Yonglong Tian, Dilip Krishnan, and Phillip Isola. Contrastive multiview coding. *arXiv preprint arXiv:1906.05849*, 2019.
- [36] Riccardo Volpi, Hongseok Namkoong, Ozan Sener, John C Duchi, Vittorio Murino, and Silvio Savarese. Generalizing to unseen domains via adversarial data augmentation. In *Advances in Neural Information Processing Systems*, pages 5334–5344, 2018.
- [37] Hal Daumé III, Abhishek Kumar, and Avishek Saha. Frustratingly easy semi-supervised domain adaptation. In *Proceedings of the 2010 Workshop on Domain Adaptation for Natural Language Processing*, pages 53–59. Association for Computational Linguistics, 2010.

A Theory and Proofs

A.1 D-separation

We first expand on the d-separation definition, providing a few examples that illustrate conditional independence implications of specific graph structures in Figure 3. We use these three conditions for all the proofs below.



(a) Chain: $A \not\perp\!\!\!\perp B$; $A \perp\!\!\!\perp B|C$ (b) Fork: $A \not\perp\!\!\!\perp B$; $A \perp\!\!\!\perp B|C$ (c) Collider: $A \perp\!\!\!\perp B$; $A \not\perp\!\!\!\perp B|C$

Figure 3: Causal graphs with the node C as a chain, fork, or a collider. By the d-separation criteria, A and B are conditionally independent given C in (a) and (b). In (c) however, A and B are independent but become conditionally dependent given C .

A.2 Proof of Proposition 1

Proposition 1. *The ERM estimator from (1) learns the true f^* , as the set of training domains $D_m = \mathcal{D}$ and number of data samples $n \rightarrow \infty$.*

Proof. Expanding on (1), the ERM estimator can be written as:

$$\begin{aligned}
 \hat{f}_{ERM} &= \arg \min_{f \in \mathcal{F}} \frac{1}{\sum_{d=1}^m n_d} \sum_{d=1}^m \sum_{i=1}^{n_d} l(y_i^{(d)}, f(\mathbf{x}_i^{(d)})) \\
 &= \arg \min_{f \in \mathcal{F}} \frac{1}{n} \sum_{d, \mathbf{x}, y \sim \mathcal{P}_m} l(y^{(d)}, f(\mathbf{x}^{(d)})) \\
 &= \arg \min_{f \in \mathcal{F}} \hat{\mathbb{E}}_{d, \mathbf{x}, y \sim \mathcal{P}_m} l(y^{(d)}, f(\mathbf{x}^{(d)})) \\
 &= \arg \min_{f \in \mathcal{F}} \hat{\mathbb{E}}_{S_n \sim \mathcal{P}_m} [l(y^{(d)}, f(\mathbf{x}^{(d)}))]
 \end{aligned} \tag{7}$$

where number of samples $n = \sum_{d=1}^m n_d$ and $S_n \sim \mathcal{P}_m(D, X, Y)$ is the training dataset of size n . Since $D_m = \mathcal{D} \Rightarrow \mathcal{P} = \mathcal{P}_m$. As $n \rightarrow \infty$,

$$\hat{f}_{ERM}^\infty = \arg \min_{f \in \mathcal{F}} \lim_{n \rightarrow \infty} \hat{\mathbb{E}}_{S_n \sim \mathcal{P}_m} l(y^{(d)}, f(\mathbf{x}^{(d)})) = \arg \min_{f \in \mathcal{F}} \mathbb{E}_{d, \mathbf{x}, y \sim \mathcal{P}} l(y^{(d)}, f(\mathbf{x}^{(d)})) = f^* \tag{8}$$

where the last equality is due to the definition of f^* in Section 2. □

A.3 Proof of Theorem 1

Theorem 1. *For a finite number of domains m , as the number of examples in each domain $n_d \rightarrow \infty$,*

1. *The set of representations that satisfy the condition $\sum_{\Omega(j,k)=1; d \neq d'} \text{dist}(\Phi(\mathbf{x}_j^{(d)}), \Phi(\mathbf{x}_k^{(d')})) = 0$ contains the optimal $\Phi(\mathbf{x}) = X_C$ that minimizes the domain generalization loss in (2).*

2. *Further, assuming that $P(X_a|O, D) < \tau < 1$ for every high-level feature X_a that is directly caused by domain, and for P -admissible loss functions [19] whose minimization is the conditional expectation (e.g., ℓ_2 loss or cross-entropy), a loss-minimizing classifier for the following loss is the true function f^* , for some value of λ .*

$$f_{\text{perfectmatch}} = \arg \min_{h, \Phi} \sum_{d=1}^m L_d(h(\Phi(X)), Y) + \lambda \sum_{\Omega(j,k)=1; d \neq d'} \text{dist}(\Phi(\mathbf{x}_j^{(d)}), \Phi(\mathbf{x}_k^{(d')})) \tag{4}$$

Proof. **CLAIM 1.** The matching condition can be written as:

$$C(\Phi) = \min_{\Phi} \sum_{d, d' \in D_m} \lim_{n_d \rightarrow \infty} \lim_{n_{d'} \rightarrow \infty} \sum_{\Omega(j,k)=1; d \neq d'} \text{dist}(\Phi(\mathbf{x}_j^{(d)}), \Phi(\mathbf{x}_k^{(d')})) \tag{9}$$

where $\Omega(j, k) = 1$ for pairs of inputs \mathbf{x}_j and \mathbf{x}_k from two different domains d and d' that correspond to the same object. The distance metric dist is non-negative, so the optimal Φ is when $C(\Phi)$ is zero.

As in the SCM from Figure 1b, let X_c represent a feature vector such that it is generated based only on the object O and that it leads to the optimal classifier in (2). From Sections 2.1 and 2.2, we know that $X_c \perp\!\!\!\perp D|O$ and that $x_c = g_{xc}(o)$. Thus, x_c is the same for inputs from the same object and we can write:

$$\text{dist}(\mathbf{x}_{c,j}^{(d)}, \mathbf{x}_{c,k}^{(d')}) = 0 \quad \forall d, d' \in D_m \text{ such that } \Omega(j, k) = 1 \quad (10)$$

Hence, $\Phi(\mathbf{x}) = \mathbf{x}_c$ leads to zero regularizer term and is one of the optimal minimizers for $C(\Phi)$.

CLAIM 2. Further, we show that any other optimal Φ is either a function of \mathbf{x}_c or a constant for all inputs. We prove by contradiction.

Let X_A represent the set of unobserved high-level features that are generated based on both the object O and the domain D . From the SCM from Figure 1b, a feature vector $X_a \subseteq X_A$ is independent of X_c given the object, $X_a \perp\!\!\!\perp X_c|O$, and $x_a = g_{xa}(d, o, \epsilon_{xa})$. Further, let there be an optimal $\Phi_a(\mathbf{x})$ for $C(\Phi)$ such that it depends on some $X_a \subseteq X_A$ (and is not trivially a constant function). Since Φ_a is optimal, $\Phi_a(\mathbf{x}_j^{(d)}) = \Phi_a(\mathbf{x}_k^{(d')})$ for all d, d' such that $\Omega(j, k) = 1$, where inputs \mathbf{x}_j and \mathbf{x}_k correspond to the same object.

Let us assume that there exists at least one object o for which the effect of domain is stochastic. That is, due to domain-dependent variation, $P(X_a = x_a | D = d, O = o) < 1$ for some d and o . Now consider a pair of inputs $\mathbf{x}_i^{(d)}$ and $\mathbf{x}_i^{(d')}$ from the same object o such that $\Omega(i, i) = 1$, and their corresponding representations are $\Phi_a(\mathbf{x}_i^{(d)})$ and $\Phi_a(\mathbf{x}_i^{(d')})$. Due to domain-dependent variation, with non-zero probability, the high-level X_a features are not the same for these two input data points, $x_{a,i}^{(d)} \neq x_{a,i}^{(d')}$. Since Φ is a deterministic function of \mathbf{x} that is not independent of X_a , if an input \mathbf{x} has a different X_a , its value of $\Phi(\mathbf{x})$ will also be different. Thus, with non-zero probability, we obtain that $\Phi(\mathbf{x}_i^{(d)}) \neq \Phi(\mathbf{x}_i^{(d')})$, unless the effect of X_a is a constant function. Hence, a contradiction and optimal Φ cannot depend on any $X_a \subseteq X_A$ that are generated based on the domain.

Therefore, an optimal solution to $C(\Phi)$ can only depend on X_c . However, any function of X_c is optimal, including trivial functions like the constant function (that will have low accuracy). Below we show that using the ERM term in (4) ensures that the optimal solution contains only those functions of X_c that also maximize accuracy.

Using (3), the empirical optimizer function can be written as (where we scale the loss by a constant $n = \sum_d n_d$, the total number of training data points):

$$\begin{aligned} \hat{f}_{pmatch} &= \arg \min_{h, \Phi} \frac{1}{n} \sum_{d=1}^m \lim_{n_d \rightarrow \infty} L_d(h(\Phi(X)), Y) \quad \text{s.t.} \quad \sum_{\Omega(j,k)=1; d \neq d'} \text{dist}(\Phi(\mathbf{x}_j^{(d)}), \Phi(\mathbf{x}_k^{(d')})) = 0 \quad (11) \\ &= \arg \min_{h, \psi} \frac{1}{n} \sum_{d=1}^m \lim_{n_d \rightarrow \infty} L_d(h(\psi(X_c)), Y) \\ &= \arg \min_f \frac{1}{n} \sum_{d=1}^m \lim_{n_d \rightarrow \infty} L_d(f(X_c), Y) \quad (12) \end{aligned}$$

where $\psi(X_c)$ denotes all functions of X_c that are optimal for (9), and the last equality is because $h \circ \psi$ can be written as $f = h \circ \psi$. Since we assume that L is a P-admissible loss function, its minimizer is the conditional expected value. Thus, for any domain d , $\arg \min_f \lim_{n_d \rightarrow \infty} \frac{1}{n_d} L_d(f(X_c), Y) = \mathbb{E}[Y|X_c, D]$. Further, by d-separation, $Y \perp\!\!\!\perp D|X_c$. Therefore, $\mathbb{E}[Y|X_c, D] = \mathbb{E}[Y|X_c]$. The above equation indicates that the loss minimizer function on any domain is independent of the domain. Thus, for the m training domains, we can write:

$$\arg \min_{f \in \mathcal{F}} \lim_{n_d \rightarrow \infty} \frac{1}{n_d} L_d(f(X_c), Y) = \arg \min_{f \in \mathcal{F}} \mathbb{E}[l(f(\mathbf{x}_c), y)] = \mathbb{E}[Y|X_c] \quad \forall d \in D_m \quad (13)$$

Now (12) can be rewritten as,

$$\hat{f}_{pmatch} = \arg \min_f \frac{1}{n} \sum_{d=1}^m \lim_{n_d \rightarrow \infty} \frac{L_d(f(X_c), Y)}{n_d} n_d = \arg \min_f \sum_{d=1}^m \lim_{n_d \rightarrow \infty} \frac{L_d(f(X_c), Y)}{n_d} \frac{n_d}{n} \quad (14)$$

From the equation above, the loss for \hat{f}_{pmatch} can be considered as a weighted sum of the average loss on each training domain where the weights are all positive. Since $\mathbb{E}[Y|X_c]$ minimizes the average loss on each domain as $n_d \rightarrow \infty$, it will also minimize the overall weighted loss for all values of the weights. Therefore, for any dataset over m domains in D_m , $\mathbb{E}[Y|X_c]$ is the optimal function that minimizes the overall loss.

Moreover, we can also write f^* as:

$$\begin{aligned} f^* &= \arg \min_{f \in \mathcal{F}} \mathbb{E}_{(d, \mathbf{x}, y)} [l(y, f(\mathbf{x}))] = \arg \min_{h \in \mathcal{F}} \mathbb{E}_{(d, \mathbf{x}, y)} [l(y, h(\mathbf{x}_c))] \\ &= \arg \min_{h \in \mathcal{F}} \mathbb{E}_{(\mathbf{x}, y)} [l(y, h(\mathbf{x}_c))] = \mathbb{E}[Y|X_c] \end{aligned} \quad (15)$$

where we utilize (13) and that the loss function is P-admissible. Hence, $f^* = \mathbb{E}[Y|X_c]$ is the loss-minimizing function for the loss in (12).

Finally, using a Lagrangian multiplier, minimizing the following soft constraint loss is equivalent to minimizing (11), for some value of λ .

$$\hat{f}_{\text{pmatch}} = \lim_{\forall d \in D_m, n_d \rightarrow \infty} \arg \min_{h, \Phi} \sum_{d=1}^m L_d(h(\Phi(X)), Y) + \lambda \sum_{\Omega(j,k)=1; d \neq d'} \text{dist}(\Phi(\mathbf{x}_j^{(d)}), \Phi(\mathbf{x}_k^{(d')})) \quad (16)$$

The result follows. \square

Comment on Theorem 1. In the case where the effect of a domain is also deterministic, it is possible that $P(X_a|O, D) = 1$ (e.g., in artificially created domains like Rotated-MNIST where every object is rotated by the *exact* same amount in each domain). In that case Theorem 1 does not apply and it is possible to learn a representation Φ_a that depends on $X_a \subseteq X_A$ and still minimizes $C(\Phi)$ to attain $C(\Phi) = 0$. For example, with two training domains on Rotated-MNIST dataset ($0^\circ, \alpha^\circ$), it is possible to learn a representation that simply memorizes to “un-rotate” the α angle back to 0° . Such a representation will fail to generalize to domains with different rotation angles, but nonetheless minimizes $C(\Phi)$ by attaining the exact same representation for each object.

In practice, we conjecture that such undesirable Φ_a are avoided by model-size regularization during training. As the number of domains increase, it may be simpler to learn a single transformation (representation) based on X_c (and independent of X_c features like angle) than learn separate angle-wise transformations for each train domain.

A.4 Proof of Corollary 1

Corollary 1. *The conditions enforced by domain-invariant ($\Phi(x) \perp\!\!\!\perp D$) or class-conditional domain-invariant ($\Phi(x) \perp\!\!\!\perp D|Y$) methods are not satisfied by the causal representation X_C . Thus, without additional assumptions, the set of representations that satisfy any of these conditions does not contain X_C , even as $n \rightarrow \infty$.*

Proof. As in the SCM from Figure 1b, let X_c represent an unobserved high-level feature vector such that it is generated based only on the object O and that it leads to the optimal classifier in (2). From Sections 2.1 and 2.2, we know that $X_c \perp\!\!\!\perp D|O$ and that $x_c = g_{xc}(o)$. Following a similar proof to Theorem 1 (Claim 1), we check whether $\Phi(\mathbf{x}) = \mathbf{x}_c$ satisfies the invariance conditions required by the two methods.

1. **Domain-invariant:** The required condition for a representation is that $\Phi_{\text{DI}}(\mathbf{x}) \perp\!\!\!\perp D$. But using the d-separation criteria on the SCM in Figure 1b, we find that $X_c \not\perp\!\!\!\perp D$ due to a path through Object O .
2. **Class-conditional domain-invariant:** The required condition for a representation is that $\Phi_{\text{CDI}} \perp\!\!\!\perp D|Y$. However using the d-separation criteria on the SCM, we find that $X_c \not\perp\!\!\!\perp D|Y$ due to a path through Object O that is not blocked by Y (nor by Y_{true} if it is observed).

Therefore, under the conditions proposed by these methods, X_c or any function of X_c is not an optimal solution without making any additional assumptions. Hence, even with infinite samples, a method optimizing for these conditions will not retrieve X_c . \square

A.5 Proof of Theorem 2

Theorem 2. *Assume that training domains are diverse such that for any two same-class inputs $\mathbf{x}_j^{(d)}$ and $\mathbf{x}_k^{(d')}$ from domains d and d' , $\text{dist}(x_{a,j}^{(d)}, x_{a,k}^{(d')}) \geq \delta_a$ where x_a is any high-level feature that is caused directly by domain. Further, assume that the distance over X_C between same-class inputs from different domains is bounded: $\text{dist}(x_{c,j}^{(d)}, x_{c,k}^{(d')}) \leq \delta_c$ and $\delta_c < \delta_a$. Then for some λ , a loss-minimizing classifier for the loss from (5) is the true function f^* , given a P-admissible loss function and a finite number of domains m with $n_d \rightarrow \infty$ in each domain.*

Proof. Since δ_c is a constant for a dataset, the loss from (5) can be written as,

$$f_{\text{randommatch}} = \arg \min_{h, \Phi} \sum_{d=1}^m L_d(h(\Phi(X)), Y) + \lambda \sum_{\Omega_Y(j,k)=1; d \neq d'} \text{dist}(\Phi(\mathbf{x}_j^{(d)}), \Phi(\mathbf{x}_k^{(d')})) - J\delta_c \quad (17)$$

where we added a scaling constant J for the total number of matches. For some value of λ , the above optimization is equivalent to,

$$\arg \min_{h, \Phi} \sum_{d=1}^m L_d(h(\Phi(X)), Y) \text{ s. t. } \sum_{\Omega_Y(j,k)=1; d \neq d'} \text{dist}(\Phi(\mathbf{x}_j^{(d)}), \Phi(\mathbf{x}_k^{(d')})) \leq J\delta_c \quad (18)$$

where δ_c is the maximum difference in X_C between two inputs with the same class but different domains.

We first show that $\Phi(\mathbf{x}) = \mathbf{x}_c$ satisfies the constraint in (18), where \mathbf{x}_c is any feature vector that is generated based only on the object ($\mathbf{x}_c = g_{x_c}(o)$), as defined in the proof of Theorem 1. Now since $\text{dist}(\mathbf{x}_{c,l}^{(d)}, \mathbf{x}_{c,i}^{(d')}) \leq \delta_c$ for any two inputs \mathbf{x}_l and \mathbf{x}_i with the same class and different domains, the constraint from (18) is satisfied by $\Phi(\mathbf{x}) = \mathbf{x}_c$.

In addition, let \mathbf{x}_a be a feature vector that is generated based on both the object and a domain ($\mathbf{x}_a = g_{x_a}(d, o, \epsilon_{x_a})$) and that is conditionally independent of \mathbf{x}_c , $X_A \perp\!\!\!\perp X_C | O$. Since we assume that $\text{dist}(\mathbf{x}_{a,l}^{(d)}, \mathbf{x}_{a,i}^{(d')}) \geq \delta_a$ and $\delta_c \leq \delta_a$, such an \mathbf{x}_a cannot satisfy the constraint in (18).

Hence, the solution to the constraint in (18) can only include \mathbf{x}_c features that are not caused by the domain (or some function of \mathbf{x}_c , $\psi(\mathbf{x}_c)$). Thus, (18) can be rewritten as,

$$\begin{aligned} &= \arg \min_{h, \psi} \frac{1}{n} \sum_{d=1}^m \lim_{n_d \rightarrow \infty} L_d(h(\psi(X_c)), Y) \\ &= \arg \min_f \frac{1}{n} \sum_{d=1}^m \lim_{n_d \rightarrow \infty} L_d(f(X_c), Y) \end{aligned} \quad (19)$$

Note that the above equation is the same as (12) from Theorem 1 proof. Following the same steps as in Theorem 1 proof, we find that $f^* = \mathbb{E}[Y|X_c]$ is the loss-minimizing classifier for (18), and hence for (5) at some value of λ . \square

B Evaluation and implementation details

In this section we describe implementation details for our proposed methods. We also discuss the evaluation protocol, including details about hyperparameters and cross-validation.

For the implementation of `ERM-RandMatch` in Eq. (5), `ERM-PerfMatch` in Eq. (4); we use the cross-entropy loss for L_d and l_2 distance for dist in Eq. (4, 5). For both methods, we consider the representation $\Phi(\mathbf{x})$ to be the last layer of the network. That is, we take h to be identity function in Eq. (4, 5) for simplicity. We use SGD to optimize for the loss for all the datasets, with details about learning rate, epoch, batch size, etc. provided in the section B.3 ahead. For all the different methods, we sample batches from the data matrix consisting of data points matched across domains; hence we ensure an equal number of data points from each source domain in a batch.

When training with `MatchDG`, for Phase-1 the architecture is selected to be ResNet-18, with the final fully connected layer removed to learn representations of dimension 512. For `MatchDG` Phase 1, the network is always the same across different datasets and irrespective of the Phase-2 architecture used for the classification task. In our evaluation, the underlying architecture for Phase 2 is kept to be the same for `ERM`, `ERM-RandMatch`, `ERM-PerfMatch`; which is set to ResNet-18 (Table 1) and LeNet (Table 6) in case of MNIST and Fashion-MNIST; while for PACS it is set to ResNet-18 (Table 4) and AlexNet (Table 11).

B.1 MatchDG implementation details

The `MatchDG` algorithm proceeds in two phases.

Initialization: We construct matches of pairs of same-class data points from different domains. Hence, given each data point we randomly select another data point with the same class from another domain. The matching for each class across domains is done relative to a base domain; which is chosen by taking the domain that has the highest number of samples for that class. This is done to avoid missing out on data points when there is class imbalance across domains. Specifically, we iterate over classes and for each class, we match data points randomly across domains w.r.t a base domain for that class. This leads to matrix \mathcal{M} of size (N', K) , where N'

refers to the updated domain size (sum of the size of base domain for all the classes) and K refers to the total number of domains. We describe the two phases below:

Phase 1: We samples batches (B, K) from the matched data matrix \mathcal{M} , where B is the batch size. For each data point x_i in the batch, we minimize the contrastive loss from (6) by selecting its matched data points across domains as the positive matches and consider every data point with a different class label from x_i to be a negative match.

After every t epochs, we periodically update the matched data matrix by using the representations learnt by contrastive loss minimization. We follow the same procedure of selecting a base domain for each class, but instead of randomly matching data points across domains, we find the nearest neighbour for the data point in base domain among the data points in the other domains with the same class label based on the L2 Distance between their representations. At the end of Phase I, we update the matched data matrix based on L2 distance over the final representations learnt. We call these matches as the *inferred* matches.

Phase 2: We train using the loss from Eq. (5), but instead of random matches, we use the inferred matches generated from Phase 1 (ERM + Inferred Match). We train the network from scratch in Phase 2 and use the representations learnt in Phase 1 to only update the matched data matrix.

The updated data matrix based on representations learnt in Phase 1 may lead to many-to-one matches from the base domain to the other domains. This can lead to certain data points being excluded from the training batches. Therefore, we construct batches such that each batch consists of two parts. The first is sampled as in Phase 1 from the matched data matrix. The second part is sampled randomly from all train domains. Specifically, for each batch (B, K) sampled from the matched data matrix, we sample an additional part of size B with data points selected randomly across domains. The loss for the second part of the batch is simply ERM, along with ERM + InferredMatch Loss on the first part of the batch.

B.2 Metrics for evaluating quality of learnt matches

Here we describe the three metrics used for measuring overlap of the learnt matches with ground-truth “perfect” matches.

Overlap %: Percentage of matches (j, k) as per the perfect match strategy Ω that are also consistent with the learnt match strategy Ω' .

$$\frac{\sum_{\Omega(j,k)=1; d \neq d'} \Omega'(j, k)}{\sum_{\Omega(j,k)=1; d \neq d'} 1} \quad (20)$$

Top-10 Overlap %: Percentage of matches (j, k) as per the perfect match strategy Ω that are among the Top-10 matches for the data point j w.r.t the learnt match strategy Ω' i.e. $S_{\Omega'}^{10}(j)$

$$\frac{\sum_{\Omega(j,k)=1; d \neq d'} \mathbb{1}[k \in S_{\Omega'}^{10}(j)]}{\sum_{\Omega(j,k)=1; d \neq d'} 1} \quad (21)$$

Mean Rank: For the matches (j, k) as per the perfect match strategy Ω , compute the mean rank for the data point j w.r.t the learnt match strategy Ω' i.e. $S_{\Omega'}(j)$

$$\frac{\sum_{\Omega(j,k)=1; d \neq d'} Rank[k \in S_{\Omega'}(j)]}{\sum_{\Omega(j,k)=1; d \neq d'} 1} \quad (22)$$

B.3 HyperParameter Tuning

To select hyperparameters, prior works [22, 26, 29] use leave-one-domain-out validation, which means that the hyperparameters are tuned after looking at data from the unseen domain. Such a setup is against the premise of the domain generalization task that assumes that a model should have no access to the test domain.

Therefore, in this work, we construct a validation set using only the source domains and use it for hyperparameter tuning. In the case of PACS, we already have access to the validation indices for each domain and use them to construct a validation set based on the source domains. For MNIST and Fashion MNIST; we construct a validation set by sampling $N/20$ (where N refers to the data points per domain for MNIST ($N = 2000$) and Fashion-MNIST ($N = 10000$) [25]) data points and then rotating them by the required angle as per the source domain. Hence, the model does not have access to the data points from the target/test domains at the time of training and validation.

For our proposed methods `ERM-PerfMatch` and `ERM-RandMatch`, there is a single hyperparameter λ to be tuned.

MNIST and Fashion MNIST In case of MNIST and Fashion MNIST, we tune λ for the approach `ERM-PerfMatch`, with access to complete source domains (15, 30, 45, 60, 75) and use the same hyper parameters for the other methods like `MatchDG` (Phase 2), `ERM`, `ERM-RandMatch`, and also for the evaluation with reduced number of domains in Table 1 and fraction of perfect matches in Table 3. The number of epochs are selected based on the convergence point for the validation dataset for each model. The details of the hyper parameters for MNIST and Fashion-MNIST are provided below: (m refers to the total number of source domains)

- **Resnet-18 (Table 1).** λ : 0.1, batch size: $16 \times m$, lr: 0.01, total epochs: 15,
- **LeNet (Table 6).** λ : 0.1, batch size: $16 \times m$, lr: 0.01, total epochs: 50

PACS. For PACS dataset, we tune a different λ for different source domains using the validation mechanism described above.

- **ResNet-18: (Table 4).** The batch size is $16 \times m$ (m refers to the total number of source domains) for all the models and learning rate is 0.001 for Photo as the target domain and 0.01 for all other target domains. The values for total epochs and λ for different training methods and target domain are given in Table 5.

Table 5: Hyper parameter tuning details on PACS with ResNet-18 architecture

		ERM	ERM-RandMatch	MatchDG(Phase 2)
Photo	Total Epochs	15	15	20
	λ	0	0.1	0.1
Art Painting	Total Epochs	15	15	15
	λ	0	0.01	0.1
Cartoon	Total Epochs	15	15	15
	λ	0	0.01	0.02
Sketch	Total Epochs	20	20	20
	λ	0	0.1	0.1

- **Alexnet: (Table 11).** The batch size is $64 \times m$, learning rate is 0.001 and total epochs 35 for all the models and target domains. For `ERM-RandMatch`, we keep the same values for batch size, learning rate and total epochs as `ERM`; while the value for λ is taken as 1.0 for all the test domains, except for the target domain Photo, where we take λ as 0.1. For `MatchDG`, the value for λ is taken as 1.0 with the batch size as $32 \times m$, learning rate as 0.001 and total epochs as 35 .

MatchDG Phase-1. The `MatchDG` Phase-1 does not have the hyper parameter (λ) as it minimizes only the contrastive loss; it however has the temperature (τ) hyper parameter. The details are provided below:

- **MNIST and Fashion MNIST.** τ : 0.5, batch size: 64, lr: 0.01, total epochs: 30
- **PACS.** τ : 0.5, batch size: 128, lr: 0.01, total epochs: 15

B.4 Reproducing Results from Prior Work

MNIST and Fashion MNIST. The results for MASF, CSD in Table 1 are taken from [25]; while the results for prior approaches in Table 6 are taken from [13]. For ResNet-18 architecture (Table 1); the results for the reduced number of domains for CSD and MASF were computed using their code which is available online¹². The MASF code was hardcoded to run for PACS dataset; which has 3 source domains that gets divided into 2 meta train and 1 meta test domain. Their code requires atleast 2 meta train domains; which leads to an issue for only 2 source domains (30, 45). In Table 1 when there are only 2 source domains; their code considers only 1 meta train domain. To resolve this issue; we create a copy of the 1 meta train domain and hence run MASF for source domains 30, 45 on MNIST.

¹<https://github.com/vihari/CSD>

²<https://github.com/biomed-mira/masf>

PACS. For the Resnet-18 architecture (Table 4), the results for CSD, JiGen are taken from [25] and the results for MASF are taken from [22]. For the AlexNet architecture (Table 11), the results for prior approaches are taken from [22]; except for IRM and ATIRL which are taken from [15].

C Additional Evaluation on Rotated MNIST and Fashion-MNIST

We present results for additional experiments on Rotated MNIST and Fashion-MNIST datasets using `MatchDG`.

C.1 Comparing `MatchDG` with prior work on the LeNet Network

Table 6 compares the accuracy results for `MatchDG` with prior work on the LeNet architecture [21]. In this setup, there are six domains in total (0° , 15° , 30° , 45° , 60° , 75°). For each test domain, the remaining five domains are used as source training domains. We observe that matching-based training methods `ERM-RandMatch` and `MatchDG` outperform prior work. They achieve accuracy almost equal to the oracle case `ERM-PerfMatch` for target angles (15° to 60°) that lie in between the source domains. For the harder extreme angles of 0° and 75° , `MatchDG` establishes new state-of-the-art accuracy results when compared to all other prior work [3, 13, 16, 21, 28].

Table 6: Accuracy for Rotated MNIST datasets using the LeNet architecture as proposed in [21]. The results for the prior approaches CCSA [21], D-MTAE [16], LabelGrad [28], DAN [3], and CrossGrad [13] are taken from Table 9 in [13].

Target	ERM	CCSA	D-MTAE	LabelGrad	DAN	CrossGrad	ERM-RandMatch	MatchDG	ERM-PerfMatch
0	85.6 (1.2)	84.6	82.5	89.7	86.7	88.3	92.1 (0.79)	93.5 (0.99)	95.7 (0.61)
15	99.5 (0.24)	95.6	96.3	97.8	98.0	98.6	99.8 (0.05)	99.8 (0.10)	99.6 (0.08)
30	98.9 (0.17)	94.6	93.4	98.0	97.8	98.0	99.5 (0.25)	99.1 (0.17)	99.6 (0.09)
45	98.7 (0.19)	82.9	78.6	97.1	97.4	97.7	99.5 (0.09)	98.9 (0.43)	99.5 (0.25)
60	99.3 (0.28)	94.8	94.2	96.6	96.9	97.7	99.5 (0.08)	99.1 (0.27)	99.5 (0.22)
75	88.4 (1.12)	82.1	80.5	92.1	89.1	91.4	92.9 (1.22)	93.1 (0.78)	96.4 (0.29)

C.2 Accuracy Results for Different Train-Test Base Images

For the domain generalization task on Rotated MNIST, prior work generates data for the unseen (test) domain by rotating the same base objects as the training domains. We evaluate `MatchDG` on a harder task where the images in the test domain are generated from base objects different than those used to generate the training domains. The Rotated-MNIST train datasets we use are the same as described in Section 4 and Table 1.

Table 7 presents the results. For all the different training domains, `MatchDG` performs better than the baseline ERM method. When the training domains are fewer (3 or 2), `MatchDG` obtains substantially higher accuracy than `ERM-RandMatch`. Compared to Table 1, when trained on the new test dataset we find that the accuracy of the oracle `ERM-PerfMatch` decreases by 1.6 points when trained over 5 domains, by 1 point when trained over 3 domains, and by 0.8 points when trained over 2 domains; indicating the relative difficulty of generalization with the new test domains. The accuracy values of `MatchDG` track those of the `ERM-PerfMatch` and show only a slight decrease in Table 7 compared to Table 1, indicating that `MatchDG` can generalize well to test domains sampled from different base objects.

Table 7: Accuracy results for Rotated MNIST dataset when the test dataset is generated from different base objects (images) than the training domains.

Source Domain	ERM	ERM+ Random	MatchDG	ERM+ Perfect
15, 30, 45, 60, 75	94.1 (0.28)	95.5 (0.47)	95.3 (0.24)	96.9 (0.19)
30, 45, 60	79.9 (2.06)	82.2 (2.59)	88.2 (1.29)	92.6 (0.25)
30, 45	64.1 (1.98)	69.2 (2.09)	79.7 (1.74)	83.4 (1.88)

C.3 Quality of representation learnt in the classification phase

In addition to Table 2 that shows metrics for Phase 1 of `MatchDG`, we compute the metrics for the classification phase (Phase 2) of `MatchDG`. Specifically, we compute the Overlap, Top-10 overlap and the Mean Rank metrics (Section B.2) for matched pairs of inputs based on the representation learnt at the end of the classification phase.

Table 8 shows the matching metrics for `MatchDG` and compares it to the matches based on the representations (last layers) learnt by the `ERM-PerfMatch` and `ERM-RandMatch` methods. For both Rotated-MNIST and Fashion-MNIST datasets, `MatchDG` obtains mean rank, Top 10 overlap and total overlap between `ERM-PerfMatch` and `ERM-RandMatch`. As the Fashion-MNIST dataset is more complex than the digits dataset, we observe that the mean rank with different training techniques is higher than the corresponding values for the Rotated-MNIST dataset.

Table 8: Mean rank, Top-10 overlap, and overlap metrics for the matches learnt in the classification phase (Phase 2), when trained on all five source domains in the Rotated MNIST and FashionMNIST datasets.

Dataset	Method	Mean Rank	Top 10 Overlap (%)	Overlap (%)
Rotated MNIST	ERM+Random	75.9 (1.49)	12.8 (0.93)	2.38 (0.38)
	MatchDG (Phase 2)	35.9 (2.24)	42.9 (2.71)	18.4 (2.13)
	ERM+Perfect (Oracle)	0.26 (0.02)	99.4 (0.08)	98.7 (0.08)
Fashion MNIST (10k)	ERM+Random	323.9 (5.05)	6.5 (0.19)	1.2 (0.02)
	MatchDG (Phase 2)	214.9 (3.26)	13.9 (0.58)	3.1 (0.22)
	ERM+Perfect (Oracle)	72.6 (1.04)	37.9 (0.54)	11.5 (0.27)

C.4 Matching metrics for Fashion-MNIST dataset with 2000 training samples per domain

In the main text (Table 2), we computed matching metrics for `MatchDG` (Phase 1) over the Fashion-MNIST dataset with 10000 samples per domain. Here we compute the same metrics for a smaller dataset with 2000 samples per domain.

We compute the metric for the default instantiation of Phase 1 of `MatchDG` initialized with random matches and compare it to an *oracle* version of `MatchDG` initialized with perfect matches. In addition, we compare the metrics for matches generated using baseline ERM (last layer of the network) in order to understand its effectiveness as a matching strategy in Phase 1. Table 9 shows the metrics for Phase 1 of `MatchDG` with 2K images from the Fashion-MNIST dataset, and reproduces the metrics for the 10K dataset from Table 2 for ease of comparison. We observe that the mean rank of perfect matches improves for the smaller dataset. Similarly, the overlap and top-10 overlap also increase for the smaller dataset. A possible reason is that there are fewer alternative matches to the perfect match as the number of samples is reduced. That said, while the overlap with perfect matches may decrease as sample size increases, the accuracy of the resultant classifier may still increase due to higher sample size.

Table 9: Metrics computed at `MatchDG` (Phase 1) for Fashion-MNIST dataset with 2K and 10K sample size used for training. Lower is better for mean rank.

Dataset	Method	Overlap (%)	Top 10 Overlap (%)	Mean Rank
Fashion MNIST (2k)	ERM	8.7 (0.14)	36.0 (1.41)	36.1 (1.66)
	MatchDG (Default)	61.5 (2.11)	88.2 (0.91)	5.9 (0.54)
	MatchDG (PerfMatch)	69.5 (10.8)	91.9 (5.8)	3.3 (2.4)
Fashion MNIST (10k)	ERM	2.8 (0.23)	13.5 (0.49)	197.2 (5.89)
	MatchDG (Default)	24.9 (3.43)	51.9 (5.63)	76.1 (14.3)
	MatchDG (PerfMatch)	58.3 (3.71)	85.3 (3.78)	10.5 (2.81)

C.5 The benefit of iterative updating of matches during Phase 1 of MatchDG

In Section 3.2, we proposed Phase 1 of the `MatchDG` algorithm with iterative updates to the computed matches. Here we compare the quality of matches learnt at the end of Phase 1 with or without using the iterative updating. Without the iterative updates, the matches always remain the same as the random matches with which the algorithm was initialized.

Table 10 shows metrics computed at the end of Phase 1 of `MatchDG` using both an iterative approach vs. a non-iterative approach. The iterative approach provides a $2\times$ and $8\times$ improvement on the overlap with perfect matches for rotated MNIST and Fashion-MNIST dataset respectively. Since higher overlap in the inferred

matches results in better classification accuracy in Phase 2 (as shown in Table 3), we conclude that using the iterative approach improves the domain generalization capability of MatchDG.

Table 10: Overlap with perfect matches. top-10 overlap and the mean rank for perfect matches for Iterative and Non Iterative MatchDG over all training domains. Lower is better for mean rank.

Dataset	Method (Phase 1)	Overlap (%)	Top 10 Overlap (%)	Mean Rank
MNIST	MatchDG(Iterative)	26.8 (2.49)	58.9 (3.31)	21.4 (2.37)
	MatchDG(Non Iterative)	14.3 (1.26)	39.9 (2.55)	36.3 (1.78)
Fashion MNIST (10k)	MatchDG(Iterative)	24.9 (3.43)	51.9 (5.63)	76.1 (14.3)
	MatchDG(Non Iterative)	3.2 (0.22)	12.4 (0.18)	248.6 (1.64)

D Evaluating MatchDG on PACS with AlexNet architecture

Finally, we compare ERM-RandMatch and MatchDG to prior work on generalization accuracy for the PACS dataset using the AlexNet architecture. As in Table 4, the task is to generalize to a test domain after training on the remaining three domains. The accuracy numbers of related work are reported from Dou et al. [22], except for IRM and ATIRL which are taken from [15].

For all test domains, Table 11 shows that both ERM-RandMatch and MatchDG outperform the baseline ERM method. Averaging over the test domains, MatchDG obtains slightly higher accuracy than ERM-RandMatch (72.3 versus 71.4). Moreover, on average MatchDG is better than 5 previous approaches [16, 6, 27, 29, 31], but some other methods like MASF [22] achieve higher accuracy than MatchDG. Since MatchDG outperforms all prior work on the same dataset when trained using ResNet-18 architecture (Table 4), we speculate that MatchDG requires a powerful underlying network architecture to use matches effectively for classification.

Table 11: Accuracy results on the PACS dataset trained with Alexnet. Comparison to prior work, D-MTAE [16], CIDDG [6], DBADG [27], MLDG [29], Epi-FCR [31], IRM [7], MetaReg [30], JiGen [26], ATIRL [15] and MASF [22].

Method/Test Domain	Photo	Art Painting	Cartoon	Sketch	Average
ERM	86.6 (0.56)	63.2 (0.56)	66.7 (0.41)	61.6 (0.67)	69.5
D-MTAE	91.12	60.27	58.65	47.68	64.45
CIDDG	78.65	62.70	69.73	64.45	68.88
DBADG	89.50	62.86	66.97	57.51	69.21
MLDG	88.00	66.23	66.88	58.96	70.71
Epi-FCR	86.1	64.7	72.3	65.0	72
IRM	89.97	64.84	71.16	63.63	72.39
MetaReg	91.07	69.82	70.35	59.26	72.62
JiGen	89.00	67.63	71.71	65.18	73.38
ATIRL	88.12	66.60	73.36	66.19	73.55
MASF	90.68	70.35	72.46	67.33	75.21
ERM-RandMatch	88.1 (0.71)	66.4 (0.40)	69.5 (0.79)	61.5 (1.25)	71.4
MatchDG	88.6 (0.56)	67.1 (0.22)	71.3 (0.12)	62.1 (0.13)	72.3